Bloch domain walls in type II optical parametric oscillators

Gonzalo Izús,* Maxi San Miguel, and Marco Santagiustina†

Instituto Mediterráneo de Estudios Avanzados, Instituto Mediterráneo de Estudios Avanzados (Consejo Superior de Investigaciones Cientificas–Universitat de les Illes Balears), E-07071 Palma de Mallorca, Spain

Received April 21, 2000

Evidence of Bloch domain walls in nonlinear optical systems is given. These walls are found in the transverse fields of optical parametric oscillators when the polarization degree of freedom, the cavity birefringence, and (or) dichroism are taken into account. These domain walls arise spontaneously and exhibit defects where Bloch walls of different chirality join together. Two dynamic regimes are found: In the first one the vector field approaches a final homogeneous state, and in the other the walls are continually generated and annihilated. This dynamic behavior is caused by the fact that walls of opposite chirality move spontaneously with opposite velocity. © 2000 Optical Society of America

OCIS codes: 190.4420, 190.4970, 190.4410

The search for novel transverse structures in nonlinear optics is actively pursued[1] because such structures may have applications in all-optical signal processing and serve as examples of pattern formation in systems away from equilibrium.[2] These structures, for example, in optical parametric oscillators (OPO's), result from the interaction of nonlinearity and diffraction in spatially extended devices such as nonlinear cavities. OPO's have been studied extensively and demonstrate that formation of patterns,[3] domain walls,[4,5] and localized structures[6] is possible. Recently, patterns were observed in a triply resonant OPO.[7]

A particularly interesting class of structure investigated is that of domain walls, i.e., fronts that connect different solutions. Ising walls are fronts for which the field vanishes at the core of the wall; they have been predicted for type I, degenerate OPO's (Ref. 4) as well as for related optical systems.[8,9] The experimental observation of walls in parametric mixing[10] and the generality of such front solutions in nonlinear optics[11] justify studies of the existence and stability of domain walls in OPO's. Although the intrinsic stability of Ising walls was recently demonstrated,[4] observation of such walls beyond the initial transient requires the presence of walk-off[5] or vortex dynamics.[12]

Besides Ising walls, another kind of front structure, i.e., Bloch walls, was investigated in systems described by a complex order parameter that satisfies an evolution equation with a broken phase invariance.[13–16] Bloch walls differ from Ising walls because in the former the field amplitude does not vanish at the core of the wall and the phase rotates by passing from one domain to the other. In this Letter we demonstrate that Bloch walls can also be formed in OPO's when cavity birefringence and (or) dichroism is accounted for.

We consider an OPO consisting of a ring cavity filled by a birefringent, nonlinear quadratic medium pumped by a uniform, external laser beam at frequency 2ω. Weak birefringence and dichroism, which account for small imperfections in the cavity, are also included in the model; for simplicity we assume that only one mirror is birefringent and dichroic. Note that the mirror's principal axes can be rotated with respect to the crystal's principal axes by an angle ϕ. In the mean field, with paraxial and single-longitudinal-mode approximations, the equations that describe the time evolution of the linear polarization components of the second-harmonic (SH) $[B_{x,y}(x, y, t)]$ and the first-harmonic (FH) $[A_{x,y}(x, y, t)]$ electric fields (where A_x and B_x are ordinary and A_y and B_y are extraordinary polarized[17]), in a type II phase-matched OPO, are

$$\partial_t B_x = \gamma_x'[-(1 + i\Delta_x')B_x + ia_x'\nabla^2 B_x + c_x' B_y + 2iK_0 A_x A_y + E_0], \quad (1)$$

$$\partial_t B_y = \gamma_y'[-(1 + i\Delta_y')B_y + ia_y'\nabla^2 B_y + c_y' B_x], \quad (2)$$

$$\partial_t A_x = \gamma_x[-(1 + i\Delta_x)A_x + ia_x\nabla^2 A_x + iK_0 A_y^* B_x + c_x A_y], \quad (3)$$

$$\partial_t A_y = \gamma_y[-(1 + i\Delta_y)A_y + ia_y\nabla^2 A_y + iK_0 A_x^* B_x + c_y A_x]. \quad (4)$$

The coefficients $\gamma_{x,y}$ and $\gamma_{x,y}'$ (cavity decay rates), $\Delta_{x,y}$ and $\Delta_{x,y}'$ (cavity detuning), and $a_{x,y}$ and $a_{x,y}'$ (diffraction coefficients) are defined as in Refs. 3 and 17; because the birefringence of the nonlinear crystal and the dichroism of the cavity, they can be slightly different from one another, even when the signal and the idler are frequency degenerate. Other parameters are nonlinearity K_0 and injected pump E_0, which for simplicity we considered to be linearly polarized along the x axis. Hence the highly mismatched component B_y is neither pumped nor nonlinearly coupled with other components. The linear coupling coefficients $c_{x,y}$ and $c_{x,y}'$ are given by

$$c_{x,y} = \frac{p + i\delta}{T \pm p\cos(2\phi)}\sin(2\phi),$$

$$c_{x,y}' = \frac{p' + i\delta'}{T' \pm p'\cos(2\phi)}\sin(2\phi), \quad (5)$$

where the plus (minus) applies for the x-(y-)polarized component. The coefficient $2p$ ($2p'$) represents the mirror dichroism, i.e., the ratio between the difference of reflectivities and the average

0146-9592/00/191454-03$15.00/0

reflectivity of the FH (SH) polarization components. The coefficient 2δ ($2\delta'$) represents the mirror birefringence, i.e., the ratio between the differential phase delay and the average delay of the FH (SH) polarization components. Finally, T (T') is the average transmittivity for the FH (SH). A linear coupling between A_x and A_y, which accounts for the insertion of intracavity wave plates in a type II OPO with no transverse spatial dependence, causing phase locking of signal and idler fields, was considered in Ref. 18. The equations that we have introduced include those of previous studies as special cases.

A linear stability analysis shows that the trivial solution $A_{x,y} = 0$, $B_x = (1 + i\Delta'_y)E_0/[1 - \Delta'_x\Delta'_y - c'_xc'_y + i(\Delta'_x + \Delta'_y)]$, $B_y = c'_yE_0/[1 - \Delta'_x\Delta'_y - c'_xc'_y + i(\Delta'_x + \Delta'_y)]$ of Eq. (1) is stable for $E_0 < E_c$, where $E_c = (1 + i\Delta_x)\sqrt{1 + \tilde{\Delta}^2}$ and $\tilde{\Delta} = (\gamma_x\Delta_x + \gamma_y\Delta_y)/(\gamma_x + \gamma_y) > 0$ if $c_{x,y} = c'_{x,y} = 0$. For $c_{x,y}$, $c'_{x,y} \neq 0$, threshold E_c could be determined only through numerical solutions; note that it decreases as the coupling strengths $|c_{x,y}|$ and $|c'_{x,y}|$ increase.

If the pump amplitude exceeds $|E_c|$, the steady state becomes unstable, and signal and idler fields are generated. For $\tilde{\Delta} > 0$ the homogeneous perturbations have the largest growth rate, and two homogeneous solutions, $A^+_{x,y}$ and $A^-_{x,y}$, of equal amplitude and phase shifted by π rad ($A^+_{x,y} = -A^-_{x,y}$), bifurcate from $A_x = A_y = 0$. They are equivalent solutions because they have the same probability of being selected starting from random initial conditions close to the unstable state. For a type II OPO we demonstrate that Bloch walls can form that are the linear coupling $c_{x,y}$, the parameters that break the phase invariance and control the transition from Bloch to Ising walls. Note that this transition has been demonstrated for a parametrically forced complex Ginzburg–Landau equation,[13,14] where the forcing amplitude is the tuning parameter. Such an equation, in the nonvariational case, resembles the model of a singly resonant, degenerate OPO but with a main difference, which actually prevents the observation of Bloch walls. In fact, the formation of Bloch walls in a parametrically forced complex Ginzburg–Landau equation requires a limitation on the strength of the parametric forcing[13] that cannot be satisfied in the case of singly resonant, degenerate OPO's.

Numerical integrations of Eq. (1) confirm that stationary uniform domains, where $A_{x,y}$ are either $A^+_{x,y}$ or $A^-_{x,y}$, form spontaneously. For small values of $c_{x,y}$ and $c'_{x,y}$, separating fronts are of the Bloch type, whereas for larger values they are of the Ising type. The trivial unstable solutions randomly perturbed by complex Gaussian white noise (delta correlated in space and time) have been set as an initial condition for integration.

Figure 1 shows a one-dimensional (1D) Bloch wall for A_x. The phase can rotate clockwise or counterclockwise in the complex plane across the interface. This characteristic is called chirality.[13] The interface shown in Fig. 1 has positive chirality (clockwise rotation); the wall for A_y has the opposite chirality.

In two dimensions (2D) the domain walls can emerge with opposite chirality in different spatial regions. The change of chirality takes place at single points where the phase field is not defined and the amplitude is zero (defects). An example of the transient transverse patterns is shown in Fig. 2, where walls of different chirality (represented by black and white curves) that we call defects are shown as black dots in the intensity field [Fig. 2(b)] and the phase field is shown in Fig. 2(c). Similar structures have been seen in the ordering process of a nonconserved two-dimensional anisotropic XY spin system.[19] The dynamics of Bloch walls in 2D depends on the detuning and damping values and is influenced by the curvature of the walls. For $\gamma_x\Delta_x = \gamma_y\Delta_y$, flat Bloch walls are stable (as one can verify by observing that 1D walls do not move for the same parameters) then, the dynamics is controlled mainly by the curvature of the fronts. This process leads to the growth of a parametrically forced complex Ginzburg–Landau equation phase and the annihilation of all the defects as in the dynamics of the two-dimensional in the variational case.[19] For $\gamma_x\Delta_x \neq \gamma_y\Delta_y$, walls of different chirality move in opposite directions in a 1D system. Then, in 2D, the defects are notably stable and the Bloch walls of different chirality tend to spiral about the defects.[14] The

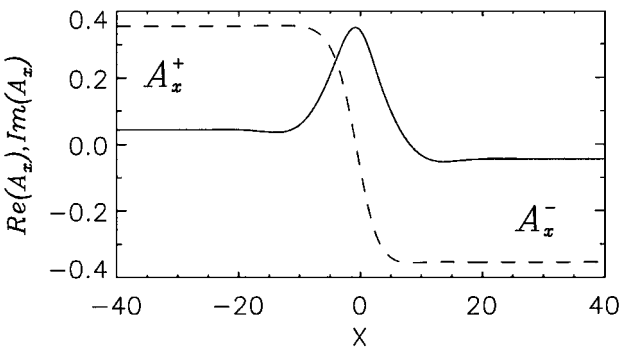

Fig. 1. Numerical solution of Eq. (1) in one spatial dimension, showing a Bloch wall. The solid (dashed) curve, the real (imaginary) part of A_x. The parameters are $\gamma_x = \gamma'_x = 1$, $\gamma_y = \gamma'_y = 1.002$, $\Delta'_x = \Delta'_y = 0$, $\Delta_x = 0.01$, $\Delta_y = 0.03$, $a'_x = a'_y = 0.125$, $a_x = a_y = 0.25$, $K_0 = 1$, $E_0 = 1.25$, $c'_{x,y} = 0.025(1 - i/2)$, and $c_{x,y} = 0.02i$. $A^\pm_x$ indicate the two possible homogeneous stable states.

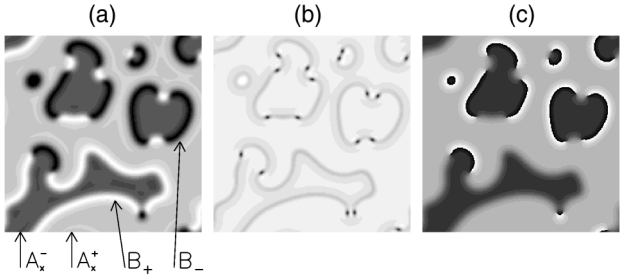

Fig. 2. Snapshot at time $t = 1600$ of the field $A_x(x, y, t)$: (a) real part, (b) intensity, (c) phase. The parameters are the same as in Fig. 1, except that $c'_{x,y} = 0.025(1 + i/2)$ and $c_{x,y} = 0.02(1 + i)$. In (a) homogeneous stable states ($A^\pm_x$) and fronts ($B_\pm$), which correspond to Bloch walls with positive–negative chirality, are labeled.

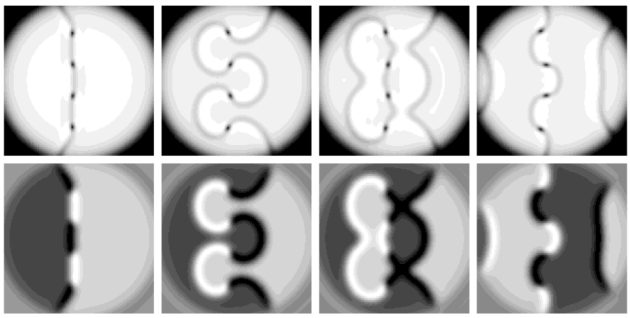

Fig. 3. Time evolution of Bloch walls; the intensity (real part) of A_x is shown above (below) for (a) $t = 0$, (b) $t = 1000$, (c) $t = 1150$, (d) $t = 1550$. The parameters are the same as in Fig. 1, except that $c'_{x,y} = 0.01$ and $c_{x,y} = 0.025$.

fronts of equal chirality are annihilated when they collide, and new ones are generated by the defects; the result is the persistent spatiotemporal complex behavior, shown in Fig. 3.

The coupling coefficients $c_{x,y}$ and $c'_{x,y}$ control the wall width and the transition from the Bloch to the Ising type. The Bloch wall width diverges to infinity as $c_{x,y} \to 0$; clearly Bloch walls are not stable for $c_{x,y} = 0$ because phase invariance is restored in Eq. (1). However, even a small amount of birefringence or dichroism is sufficient to make these structures stable, and therefore they are likely to be observed in type II OPO's as a result of any weak imperfection of the cavity. For $c_{x,y} = 0$, Ising walls are not stable either; however, they become stable and form spontaneously for larger values of $|c_{x,y}|$ for which Bloch walls lose their stability. Beyond the Bloch–Ising transition, labyrinthine patterns are formed[9,10] because flat Ising walls are modulationally unstable, i.e., tend to increase their curvature like those found for intracavity SH generation.[8]

In conclusion, we have demonstrated that Bloch walls can be found as transverse structures of type II optical parametric oscillators. They appear when there is weak linear coupling between the signal and the idler fields. Two-dimensional Bloch walls are characterized by sections of different chirality, separated by phase defects at which the field amplitude is zero. Two dynamic regimes, which depend on the decay rates and the detunings, are found: In the first, the wall dynamics is dominated by the curvature and a final homogeneous state is reached; in the second, the walls spiral about the stable defects, and a persistent creation and annihilation of fronts is observed. The transition from Bloch to Ising walls was observed when the linear coupling strength was increased.

This study was supported by European Commission project QSTRUCT (FMRX-CT96-0077) and by Direccíon General de Investigación Cientifica y Técnica (Spain) project PB94-1167. The authors acknowledge helpful discussions with G.-L. Oppo and L. Palmieri. The authors' URL is http://www.imedea@uib.es.PhysDept.

*Permanent address, Departamento de Física, Facultad de Ciencias Exactos y Naturales, Universidad Nacional de Mar del Plata, Argentina, and Consejo Nacional de Investigaciones Científicas y Tecnología.

†Permanent address, Istituto Nazionale di Fisica della Materia, Dipartimento di Elettronica e Informatica, Università di Padova, Padua, Italy, e-mail address, marco@wave.dei.unipd.it.

References

1. G. De Valcárcel, E. Roldan, and R. Vilaseca, J. Opt. B. **1,** 19–197 (1999).
2. M. C. Cross and P. C. Hohenberg, Rev. Mod. Phys. **65,** 851 (1993).
3. G.-L. Oppo, M. Brambilla, and L. A. Lugiato, Phys. Rev. A **49,** 2028 (1994).
4. S. Trillo, M. Haelterman, and A. Sheppard, Opt. Lett. **22,** 970 (1997); S. Longhi, Phys. Scr. **56,** 611 (1997); N. Kutz, T. Ernaux, S. Trillo, and M. Haelterman, J. Opt. Soc. Am. B **16,** 1936 (1999).
5. M. Santagiustina, P. Colet, M. San Miguel, and D. Walgaef, Opt. Lett. **23,** 1167 (1998).
6. K. Staliunas and V. Sánchez-Morcillo, Phys. Rev. A **57,** 1454 (1998); G. L. Oppo, A. J. Scroggie, and W. J. Firth, J. Opt. B **1,** 133 (1999); B. M. Le Berre, D. Leduc, E. Ressayre, and A. Tallet, J. Opt. B **1,** 153 (1999).
7. M. Vaupel, A. Matre, and C. Fabre, Phys. Rev. Lett. **83,** 5278 (1999).
8. U. Peschel, D. Michaelis, C. Etrich, and F. Lederer, Phys. Rev. E **58,** R2745 (1998).
9. R. Gallego, M. San Miguel, and R. Toral, Phys. Rev. E **61,** 2241 (2000).
10. V. Taranenko, K. Staliunas, and C. Weiss, Phys. Rev. Lett. **81,** 2236 (1998).
11. N. N. Rozanov, in *Progress in Optics*, E. Wolf, ed. (Pergamon, London, 1996), Vol. 35, p. 1.
12. G.-L. Oppo, A. J. Scroggie, and W. J. Firth, in *European Quantum Electronic Conference* (Institute of Electrical and Electronics Engineers, New York, 1998), p. 245.
13. P. Coullet, J. Lega, B. Houchmanzadeh, and J. Lajzerowicz, Phys. Rev. Lett. **56,** 1352 (1990).
14. T. Frisch, S. Rica, P. Coullet, and J. M. Gilli, Phys. Rev. Lett. **72,** 1471 (1994).
15. S. Longhi, Europhys. Lett. **37,** 257 (1997).
16. I. P. Arjona, F. Silva, V. Sanchez-Morcillo, E. Roldan, and S. G. Valcárcel, Departament d'Òptica, Universitat de València, València, Spain.
17. G. Izús, M. Santagiustina, M. San Miguel, and P. Colet, J. Opt. Soc. Am. B **16,** 1592 (1999).
18. C. Fabre, E. Mason, and N. Wong, Opt. Commun. **170,** 299 (1999), and references therein.
19. H. Tutu, Phys. Rev. E **56,** 5036 (1997).